

An alternative scattering method to characterize surface roughness from transparent substrates

M. Zerrad, C. Deumié, M. Lequime, and C. Amra

Institut Fresnel, UMR CNRSTIC 6133 Université Paul Cézanne, EGIM, Université de Provence Domaine Universitaire de St Jérôme 13397 Marseille Cedex 20, France

myriam.zerrad@fresnel.fr

<http://www.fresnel.fr>

Abstract: An alternative scattering method is developed to characterize surface roughness from the two faces of transparent substrates. Specific weights are attributed to each surface in the scattering process, due to the large substrate thickness. The resulting roughness spectra are shown to quasi-overlap those of near field microscopy.

© 2006 Optical Society of America

OCIS codes: (120.5820) Scattering measurements; (120.6660) Surface measurements, roughness

References and links

1. J. M. Elson and J. M. Bennett, "Relation between the angular dependence of scattering and the statistical properties of optical surfaces," *J. Opt. Soc. Am.* **69**, 31-47 (1979).
2. J. M. Bennett, "Comparison of techniques for measuring the roughness of optical surfaces," *Opt. Eng.* **24**, 380-387 (1985).
3. C. Amra, "From light scattering to the microstructure of thin-film multilayers," *Appl. Opt.* **32**, 5481-5491 (1993).
4. C. Amra, C. Grezes-Besset, P. Roche, and E. Pelletier, "Description of a scattering apparatus: application to the problems of characterization of opaque surfaces," *Appl. Opt.* **28**, 2723-2730 (1989).
5. O. Kienzle, J. Staub, and T. Tschudi, "Light scattering from transparent substrates: theory and experiment," *Phys. Rev. B* **50**, 1848-1860 (1994).
6. M. Zerrad, C. Deumié, M. Lequime, C. Amra, and M. Ewart, "Light-scattering characterization of transparent substrates," *Appl. Opt.* **45**, 1402-1409 (2006).
7. P. Kadkhoda, A. Muller, D. Ristau, A. Duparre, S. Glied, H. Lauth, U. Schuhmann, N. Reng, M. Tilsch, R. Schuhmann, C. Amra, C. Deumie, C. Jolie, H. Kessler, T. Lindstrom, C. G. Ribbing, and J. M. Bennett, "International round-robin experiment to test the International Organization for Standardization total-scattering draft standard," *Appl. Opt.* **39**, 3321-3332 (2000).
8. J. M. Elson, "Theory of light scattering from a rough surface with an inhomogeneous dielectric permittivity," *Phys. Rev. B* **30**, 5460-5480 (1984).
9. C. Amra, G. Albrand, and P. Roche, "Theory and application of antiscattering single layers: antiscattering antireflection coatings," *Appl. Opt.* **25**, 2695-2702 (1986).
10. C. Amra, "Light scattering from multilayer optics. Part A: Investigation tools," *J. Opt. Soc. Am. A* **11**, 197-210 (1994).
11. C. Amra, "Light scattering from multilayer optics. Part B: Application to experiment," *J. Opt. Soc. Am. A* **11**, 211-226 (1994).
12. J. M. Elson, J. P. Rahn, and J. M. Bennett, "Relationship of the total integrated scattering from multilayer-coated optics to angle of incidence, polarization, correlation length, and roughness cross-correlation properties," *Appl. Opt.* **22**, 3207-3219 (1983).
13. C. Amra, C. Grezes-Besset, and L. Bruel, "Comparison of surface and bulk scattering in optical multilayers," *Appl. Opt.* **32**, 5492-55503 (1993).
14. A. Duparre and S. Kassam, "Relation between light scattering and the microstructure of optical thin films," *Appl. Opt.* **32**, 5475-5480 (1993).
15. C. Amra, D. Torricini, and P. Roche, "Multiwavelength (0.45-10.6 μ m) angle-resolved scatterometer or how to extend the optical window," *Appl. Opt.* **32**, 5462-5474 (1993).
16. O. Gilbert, C. Deumie, and C. Amra, "Angle-resolved ellipsometry of scattering patterns from arbitrary surfaces and bulks," *Opt. Express* **13**, (2005).
17. C. Deumie, R. Richier, P. Dumas, and C. Amra, "Multiscale roughness in optical multilayers: atomic force microscopy and light scattering," *Appl. Opt.* **35**, 5583-5594 (1996).
18. P. Dumas, B. Bouffakhreddine, C. Amra, O. Vatel, E. Andre, R. Galindo, and F. Salvan, "Quantitative microroughness analysis down to the nanometer scale," *Europhys. Lett.* **22**, 717-722 (1993).

1. Introduction

Angle-resolved light scattering has been extensively described as a powerful tool to characterize surface roughness of micro-polished [1-4] substrates. However the technique has always been limited to the case of opaque substrates [4] such as black or colored glasses, metals and semiconductors. Indeed in the case of transparent substrates [5-7], both front and back surfaces scatter the incident light so that these surfaces cannot be separately characterized in the far field pattern. One solution was recently proposed [6] to solve this point and is based on a confocal analysis, but suffers difficulties due to the angular range of validity connected with substrate thickness. In this paper we propose an alternative solution which may be of critical interest when optical characterization is required. In particular the method involves standard scattering measurements with no use of additional devices.

2. Theory

2.1 Scattering equations and formulae

For a single surface (Fig. 1) whose irregularities are assumed to be much smaller than the illumination wavelength, a simple relationship issued from first-order theory [8, 9] allows to determine the statistical surface properties from the measurement of the scattering pattern. The measurement of the scattering intensities $I^-(\theta_0, \phi)$ and $I^+(\theta_s, \phi)$, respectively in the reflected and transmitted space (Fig. 1) are connected with the roughness spectrum thanks to the formula [1, 10, 11]:

$$I^\pm(\theta, \phi) = C^\pm(\theta, \phi) \gamma(\theta, \phi) \quad (1)$$

with θ and ϕ respectively the normal and polar angles that describe a scattering direction in the far field, and $C^\pm(\theta, \phi)$ an optical factor connected with material index, polarization and wavelength, directions. The roughness spectrum of the surface is denoted $\gamma(\theta, \phi)$ and describes the Fourier Transform of the surface profile autocorrelation function. It can be written as the square modulus of the Fourier Transform of the surface topography $\hat{h}(\vec{\sigma})$ by the relation:

$$\gamma(\vec{\sigma}) = \frac{4\pi^2}{S} |\hat{h}(\vec{\sigma})|^2 \quad (2)$$

with S the illuminated area.

It is also practical to use a one dimensional spectrum curve given by the following polar average:

$$\bar{\gamma}(\theta) = \bar{\gamma}(\sigma) = \frac{1}{2\pi} \int_{\phi=0}^{2\pi} \gamma(\theta, \phi) d\phi \quad (3)$$

with the spatial pulsation ($\vec{\sigma}$) and frequency ($\vec{\nu}$):

$$\sigma = |\vec{\sigma}| = \frac{2\pi}{\lambda} \sin \theta = 2\pi\nu \quad (4)$$

Notice that the angular intensity given in (1) is not different from the Poynting flux per unit of solid angle. The root mean square of roughness (δ in nm units) can be derived from the integration of the roughness spectrum (γ in nm^4 units) in the frequency or angular range as follows:

$$\begin{aligned}
 \delta^2 &= \int_{\bar{\sigma}} \gamma(\bar{\sigma}) d\bar{\sigma} \\
 &= 2\pi \int_{\sigma_{\min}}^{\sigma_{\max}} \sigma \bar{\gamma}(\sigma) d\sigma \\
 &= \frac{2\pi n_0}{\lambda} \int_{\Phi=0}^{2\pi} \int_{\theta_{\min}}^{\theta_{\max}} \gamma(\theta, \Phi) \sin \theta \cos \theta d\theta d\Phi
 \end{aligned} \tag{5}$$

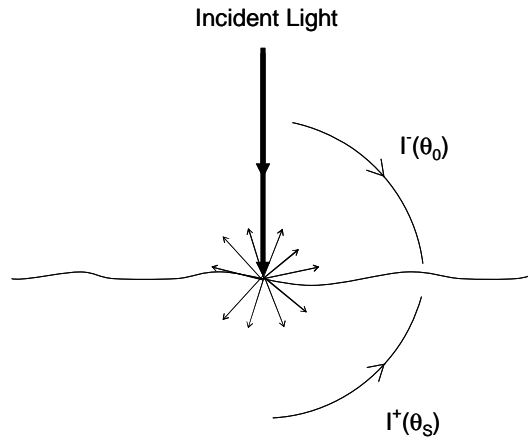


Fig. 1. Light scattering from a single interface

In the case of a transparent substrate (Fig. 2), both front and back surfaces simultaneously scatter the incident light. In this case relation (1) must first be completed to take into account angle resolved scattering from each surface, and its multiple incoherent reflections in the substrate. If we consider that interfaces (0) and (1) designate the top and back surfaces respectively, the angular intensity I_r scattered by the transparent substrate in the reflected half space is given by:

$$I_r(\theta_0, \phi) = \left\{ C_0^-(\theta_0) + C_0^+(\theta_s) \frac{R(\theta_s)}{1 - R^2(\theta_s)} \beta(\theta_s) \right\} \gamma_0(\theta, \phi) + C_1^-(\theta_s) \frac{1}{1 - R^2(\theta_s)} \beta(\theta_s) \gamma_1(\theta, \phi) \tag{6}$$

with $C_i^-(\theta_0)$ the optical factor in reflection for interface (i), $C_i^+(\theta_s)$ the optical factor in transmission for interface (i), γ the roughness spectrum of surface (i), R the specular reflection factor of interface (0) or (1) at incidence θ_s in the substrate, and β a factor for description of diffuse transmittance:

$$\beta(\theta_s) = T(\theta_s) \left(\frac{n_0}{n_s} \right)^2 \frac{\cos \theta_0}{\cos \theta_s} \quad (7)$$

with T the classical transmission factor of the interfaces for specular fluxes. In this paper the substrate absorption is assumed to be negligible. Moreover, normal illumination is assumed with natural light, for which reason the optical coefficients $C_i^\pm(\theta)$ does not depend on polar angle. We may notice in this section that we did not consider interferences between waves scattered from the two interfaces, because the interface roughnesses are assumed to be not correlated, since they result from a polishing process at each substrate side.

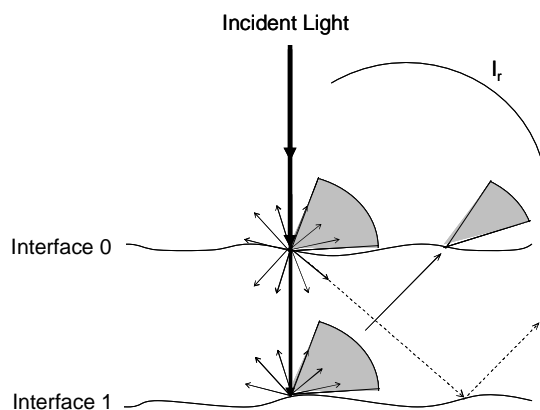


Fig. 2. Scattering from the two surfaces of a transparent substrate

2.2 Specific weights at each interface

One difficult question now concerns the relative weight that should be attributed to each interface in the scattering process, in addition to the roughness weight. Indeed Eq. (1) that we use for angular scattering is valid for single surfaces that bound a semi-infinite medium, while the sample under study here is a substrate. In order to find a rigorous result for the excitation weight at each interface of a thick substrate, it is first necessary to come back to scattering from thin films and consider the theory [12-14] that was developed to predict angular scattering from multilayers. The present case is the simplest one since we only have to consider a single layer given by the glass substrate, between air (substrate) and air (superstrate). Therefore the two interface roughnesses are excited by the E_i values of the stationary zero-order field at the two surfaces (i). At normal illumination, these E_i values depend on the phase parameter given by $\eta = (2\pi/\lambda) ne$, with ne the optical thickness of the layer. The result is that angular scattering at a particular direction is proportional to the square modulus of the excitation field, and to the roughness spectrum at the adequate spatial frequency. However, due to the large substrate thickness, it is also necessary to calculate an average of the excitation terms as follows:

$$\alpha_i = \frac{\langle |E_i|^2 \rangle}{\Phi_0^+} \quad (8)$$

with Φ_0^+ the incident flux on the substrate, and the brackets $\langle \rangle$ designate an average value over phase terms η due to the large substrate thickness. With this procedure and after tedious but direct analytical calculation, the average excitation factor α_i for each surface of a thick substrate is found to be:

$$\alpha_0 = 1 + 2 \left(r_s + \frac{R_s}{1 + R_s} \right) \quad \text{with } r_s = -\sqrt{R_s} \quad (9)$$

$$\alpha_1 = \frac{1 - R_s}{1 + R_s} = \frac{T_s}{1 + R_s} \quad (10)$$

with R_s and T_s the reflection and transmission factors for a single air/glass interface. Notice that the α_1 weight at surface (1) is given by the average value ($T^* = \alpha_1$) of the substrate transmission factor over phase terms due to the large substrate thickness, which can be classically calculated via incoherent multiple reflections. At the inverse, the α_0 weight of the top interface cannot be predicted from multiple incoherent reflections and differs from the value $(1 + R^*)$, with $R^* = 2R_s/(1 + R_s)$ the incoherent reflection of the substrate. To give an order of magnitude, if we consider a glass substrate in the air (with $n_0 = 1$ and $n_1 = 1.5$) illuminated at $\lambda = 633$ nm, we obtain in the case of a glass substrate: $\alpha_0 = 0.677$ and $\alpha_1 = 0.923$. These values emphasize the weight of these coefficients and their noticeable departure from unity. They cannot be neglected in the characterization method that follows.

3. Characterization method

The method is based on a simple approach involving classical scattering measurements by reflection, with two specific measurement configurations. In the first configuration interface 0 is the top surface, while in the second situation interface 1 is the top surface (Fig. 3).

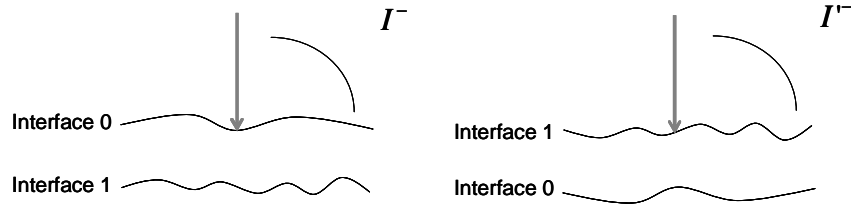


Fig. 3. Scattering measurements by reflection for two specific configurations

In the first situation angular scattering by reflection is given as:

$$I^- = D_0^- \gamma_0 + D_1^- \gamma_1 \quad (11)$$

where the coefficients D_i^- are given from relation (6-11):

$$D_0^- = \left(C_0^-(\theta_0) + C_0^+(\theta_s) \frac{R(\theta_s)}{1 - R^2(\theta_s)} \beta(\theta_s) \right) \alpha_0 \quad (12)$$

$$D_1^- = \left(C_1^-(\theta_s) \frac{1}{1 - R^2(\theta_s)} \beta(\theta_s) \right) \alpha_1 \quad (13)$$

The second situation leads to similar equations with identical coefficients, except that the spectra are inverted:

$$I^- = D_0^- \gamma_1 + D_1^- \gamma_0 \quad (14)$$

Therefore Eqs. (11) and (14) allow to solve the system and reach the basic result:

$$\gamma_0 = \frac{D_0^- I^- - D_1^- I'^-}{(D_0^-)^2 - (D_1^-)^2} \quad (15)$$

and

$$\gamma_1 = \frac{D_0^- I'^- - D_1^- I^-}{(D_0^-)^2 - (D_1^-)^2} \quad (16)$$

These last relations allow separation of the 2 faces and the determination of each roughness spectrum in the whole angular range, provided that the sensitivity of the method is adequate. Notice that the spectra could also be obtained from the two scattering curves by transmission (I^+ and I'^+) or from the scattering curves from both reflection and transmission (I^- and I'^+). In the general case where all measurements can be used, the two spectra can be measured and inter-checked.

4. Application

In order to test the method, we used a 9 mm thick fused silica sample with standard polish quality. Light scattering measurements were performed for the two situations of Fig. 3, that is, before and after inversion of the interfaces. A well-known scatterometer [15, 16] was used to record all data, with a relative accuracy better than 1 %. The wavelength under study is $\lambda = 633\text{nm}$.

The measured roughness spectra are plotted in Fig. 4 for the 2 surfaces, versus spatial pulsation $\sigma = (2\pi/\lambda) \sin\theta$. The roughnesses were obtained by integration of the spectra in the angular scattering range, with the result:

$$\delta_0 = 0.48 \text{ nm} \text{ and } \delta_1 = 0.56 \text{ nm}$$

For comparison we have also plotted in Fig. 4, the spectra that would be obtained without our separation method, that is, under the assumption of a single interface of a semi-infinite substrate. The difference is noticeable since the roughness values are increased as:

$$\delta_0 = 0.91 \text{ nm} \text{ and } \delta_1 = 0.85 \text{ nm}.$$

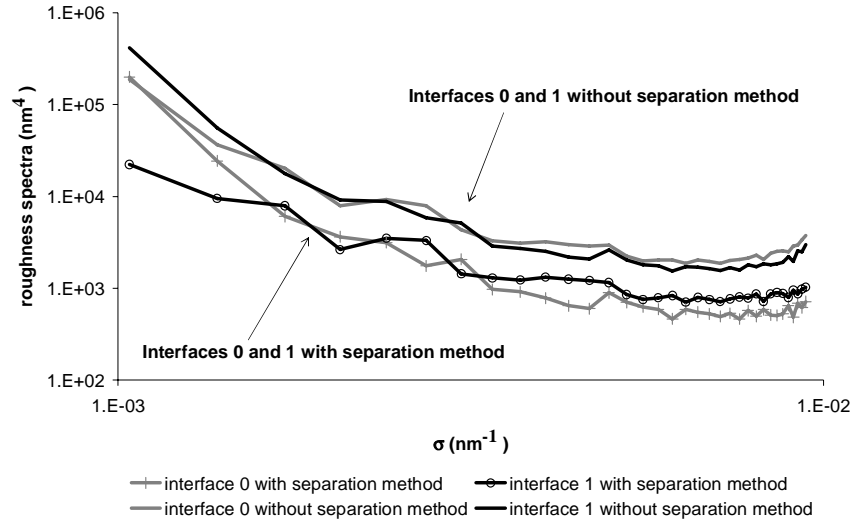


Fig. 4. Roughness spectra determined with and without the separation method

5. Comparison with near field microscopy

In order to validate the method, extra verifications can be performed thanks to atomic force microscopy, as was shown by previous works [17]. The topography of each substrate surface was recorded with AFM, then, we calculated their two-dimensional Fourier transforms, and we deduced from it, with relation (2), the roughness spectra $\gamma(\theta, \phi)$. In a second step we averaged the spectra over polar angle ϕ [17, 18] in order to reach single one-dimensional curves. These last spectra can then be compared to the spectra that were determined with our scattering separation technique.

However it is necessary to take into account the frequency band-passes for each measurement technique [17, 18]. In the case of light scattering, the maximum frequency is given by the inverse wavelength that corresponds to the grazing observation at $\theta = 90^\circ$, while the minimum frequency is connected with the minimum scattering angle θ_{\min} for the measurements. Concerning the AFM bandpass, it is given by the Shannon/Niquist criteria, with a minimum and maximum frequency given by:

$$\begin{aligned} \nu_{\min} &= \frac{1}{L} \\ \nu_{\max} &= \frac{1}{2\Delta x} \end{aligned} \quad (17)$$

with Δx the sampling interval and L the scan length on the sample. Therefore the band-passes are different for angle resolved scattering (B_{ARS}) and for microscopy (B_M), and given in terms of pulsations σ as:

$$B_{ARS} = \left(\frac{2\pi \sin \theta_{\min}}{\lambda}, \frac{2\pi}{\lambda} \right) \quad (18)$$

with λ the incident wavelength and θ_{\min} the minimum scattering angle, and:

$$B_M(\Delta x) = \left(\frac{2\pi}{L}, \frac{\pi N}{L} \right) \quad (19)$$

with L^2 the measured area, Δx the sampling interval and N^2 the number of data points.

A 9 mm thick fused silica sample was considered for this comparison. Parameters $L = 16 \mu\text{m}$ and $N = 300$ data points were chosen to obtain similar band-passes from the two techniques. The AFM microscopy results are presented in Fig. 5 for the interface 0 and on Fig. 6 for the interface 1. All spectra are plotted versus spatial pulsation σ . In these figures we have also plotted the results obtained with the scattering technique, with and without the separation method.

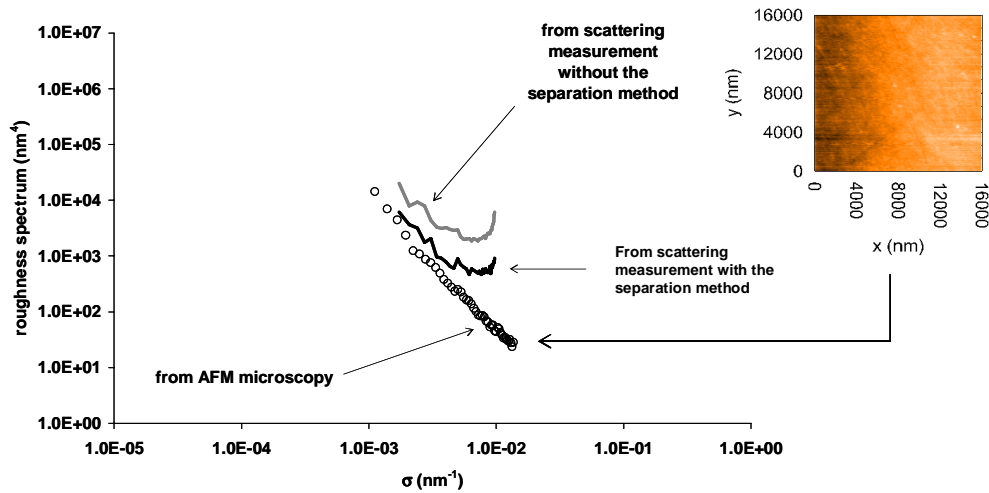


Fig. 5. Roughness spectra of interface 0 measured with AFM microscopy and light scattering, with and without the separation method.

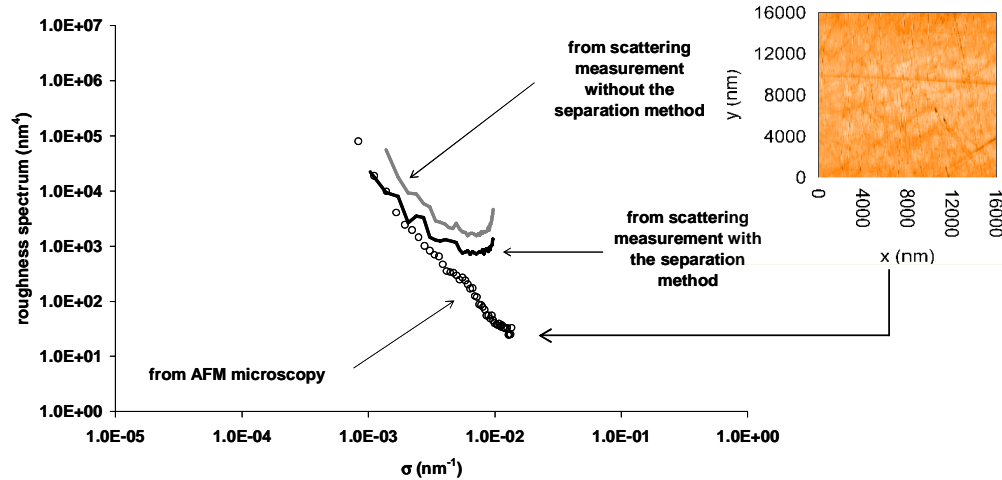


Fig. 6. Roughness spectra of interface 1 measured with AFM microscopy and light scattering, with and without the separation method.

We can see on these graphs that the roughness spectra deduced from scattering measurements with the separation method are in good agreement with the AFM spectra, in particular at low frequencies. At the inverse, the spectra calculated without the separation method are much higher than the AFM spectra. Therefore these results constitute a first interesting validation. However we also notice the departure between the AFM and separation method spectra, in particular at high frequencies. Such disagreement is due to a classical difference between near field microscopy and scattering measurements, connected with the stationarity of topography. Indeed a scattering measurement considers a surface larger than an AFM measurement (in our case, 2mm diameter versus a $16\ \mu\text{m} \times 16\ \mu\text{m}$ square). Due to the presence of localized defects (pits, dusts) on the samples, the scattering levels at large angles are greater than those of the intrinsic roughness scattering [19], while the AFM sampling procedure does not necessarily detect these localized defects because of the limited scan length.

In order to illustrate this difference, we have simulated in Fig. 7 the AFM measurement of a large surface in the presence and in the absence of localized defects. Roughness spectra and AFM pictures are given in the same figure. The results clearly show that the increase of the spectra at high frequencies is due to the presence of localized defects that cannot be seen with the AFM, which explains the remaining differences between the AFM technique and our separation method.

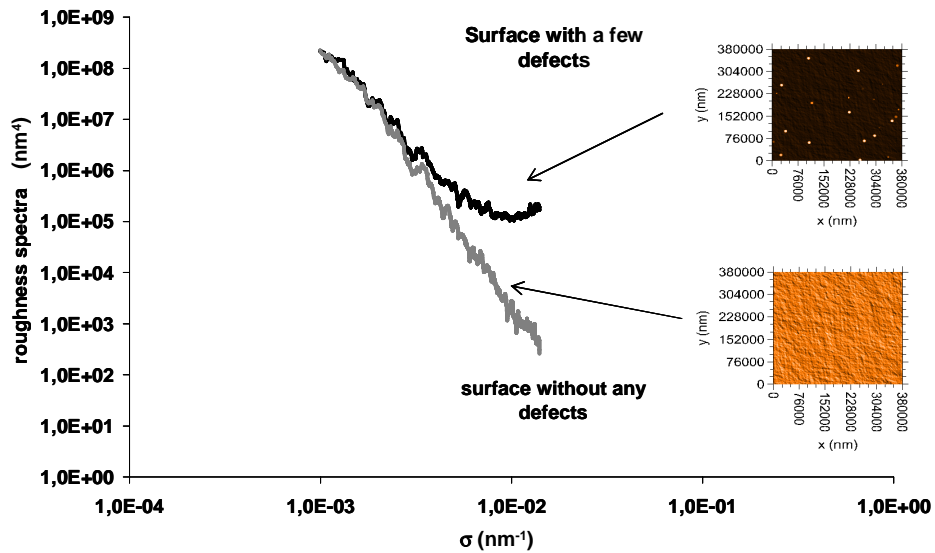


Fig. 7. Roughness spectra deduced from simulated surfaces with and without any localized defects. The units of σ and γ are respectively nm^{-1} and nm^4 .

6. Conclusion

We have validated a scattering procedure to characterize the roughness of both faces of a transparent substrate. The method involves classical measurements by reflection, for two substrate positions. It was shown to be successful provided that specific average coefficients are calculated for the weight of each interface, and extra-validation was performed with AFM microscopy. All results demonstrate that angle resolved light scattering allows the characterization of transparent substrates, which overcomes the limitation to opaque surfaces. Notice however that high accurate measurements are necessary for the method to work, including elimination of parasitic light from the side faces of the substrate.